Langmuir

Article

pubs.acs.org/Langmuir

Spectroscopy and Fluorescence Lifetime Imaging Microscopy To Probe the Interaction of Bovine Serum Albumin with Graphene Oxide

Jagannath Kuchlyan, Niloy Kundu, Debasis Banik, Arpita Roy, and Nilmoni Sarkar*

Department of Chemistry, Indian Institute of Technology, Kharagpur 721302, WB, India

Supporting Information

ABSTRACT: The interaction of graphene oxide (GO) with bovine serum albumin (BSA) in aqueous buffer solution has been investigated with various spectroscopic and imaging techniques. At single molecular resolution this interaction has been performed using fluorescence correlation spectroscopy (FCS) and fluorescence lifetime imaging microscopy (FLIM) techniques. The conformational dynamics of BSA on GO's influence have been explored by FCS and circular dichroism (CD) spectroscopy. For the FCS studies BSA was labeled covalently by a fluorophore, Alexa Fluor 488. On the addition of GO in phosphate buffer of 10 mM at pH 7.4 the diffusion time (τ_D) and the hydrodynamic radius (R_h) of BSA increase due to adsorption of BSA. Conformational relaxation time components of native BSA drastically vary with the addition of GO, signifying the change of conformational dynamics of BSA after addition of GO. The adsorption isotherm also indicates significant adsorption of BSA on the GO surface. Adsorption of BSA on the GO surface has shown in direct images of atomic force microscopy (AFM) and FLIM. Fluorescence quenching study of BSA with addition of GO also indicates that there is strong interaction between BSA and GO.

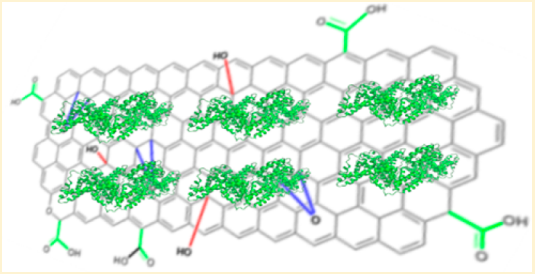

1. INTRODUCTION

In order to determine the biocompatibility, potential utilities, and applications of novel nanomaterials in biological systems, a fundamental understanding about the interactions of nanostructured materials in biological systems is essential.[1−3] For protein modulation, a number of nanomaterials with varying shapes and sizes have been utilized as substrates. These materials, due to their immense applications in body, including cells and organelles, have high potential to be used in new medicinal approaches.[4−8] Despite the fast development in science and technology, the interaction of GO with biological systems has not been studied extensively. So it is very much essential to study the protein−GO interaction in order to understand the influence of GO on structure and activities of proteins.

GO is formed by the oxidation of graphite and is a water-soluble material. It has been extensively used in the fields of biomedicine and technology, such as in diagnostics, treatment, and novel functional materials.[9,10] Because of the presence of both ionic groups and aromatic domains in GO, it is widely used in the biochemical sensing applications. GO has the ability to bridge with the substrate molecules through the formation of noncovalent bonds like hydrogen bonding, hydrophobic, $\pi-\pi$ stacking, and electrostatic interactions. Preferential interaction of GO with single-stranded (ss) nucleic acids is known to occur through hydrogen bonding and π-stacking interactions between nucleobases and the GO surface. But, in cases of double-stranded (ds) form, such binding of GO surface to the DNA base is prohibited inside the double-helical structure.[11,12] Kim et al.,[13] in their studies on the interaction of single- and double-stranded DNAs with GO, showed that GO interacts preferentially with ssDNA, although, dsDNA can also be adsorbed on GO surface with lower affinity. It is well established that GO works well in the case of immobilization of enzyme on nanostructure materials.[14,15] The role of GO as an enzyme inhibitor to regulate the activity of α-chymotrypsin has been reported by De et al.[16] Recent reports by Li et al.[17] show strong adsorption of milk protein lysozyme on GO surface. This interaction is so strong that the subsequent elimination and separation of lysozyme from the surface of GO becomes impossible. However, another investigation has also shown the decrease in the biological activity of horseradish peroxidase (HRP) after interaction with GO.[18] The immobilization of enzymes, in the absence of any surface modification or coupling reagents, occurs through the oxygen-containing groups on GO. Although there are reports regarding the GO and biomacromolecules (amino acids, peptides, biomembranes, enzymes, and proteins) interactions, no study has yet been carried out at single molecular resolution.[19−22]

FCS is an important technique that records the variations in fluorescence intensity due to the movement of fluorescent probe in a focal spot area at a single molecular level.[23−28] Fluorescence fluctuations in a small observation volume are measured in FCS, keeping the system under thermodynamic

Received: September 30, 2015
Revised: December 5, 2015
Published: December 8, 2015

DOI: 10.1021/acs.langmuir.5b03648
Langmuir 2015, 31, 13793−13801

equilibrium. FCS is a well-known technique to study biomolecular interactions, aggregation, and conformational dynamics in proteins at single-molecule resolution.[29−37] Even FCS can be employed to record the time scale regarding the conformational fluctuation of a protein. Chattopadhyay et al.[38] utilized conformational dynamics study of a fatty acid binding protein to record a single conformational relaxation time. Using FCS, Bhattacharyya and co-workers[33,34] reported the effect of room temperature ionic liquids (RTILs) on the conformational dynamics of human serum albumin (HSA) and the respiratory protein horse heart cytochrome *c*. Increased size and, consequently, slowed down protein dynamics in the native state, on addition of RTILs, were revealed from these studies. Here, BSA was used as a model protein because of its relatively high structural stability and large applications in molecular biology. Recently, Xing et al.[39] studied the BSA and lysozyme adsorption on the modified carbon nanotubes (CNTs). They demonstrated that interaction with the CNTs resulted in diminished secondary structure of protein. Chattopadhyay and co-workers established the influence of arginine on aggregation and conformation of BSA.[40] The same group also reported the urea-induced unfolding transition of a model protein, BSA, and effect of crowded environment (polyacrylamide gel) on that protein conformation. They also demonstrated the significant enhancement in the R_h of the Alexa 488-labeled protein inside the polyacrylamide gel.

Although there are several reports on the effect of GO on protein in the literature, the influence of GO on the conformational dynamics and folding of a covalent probe tagged protein has never been studied using single molecule spectroscopy (SMS). In this study, we have conducted the adsorption of BSA on GO surface in phosphate buffer at pH 7.4, and the consequent changes in the secondary structure of BSA were analyzed. This study helps us to assimilate the mechanism of adsorption of protein on GO and thus increase the scope for biomedical application of GO. For this, FCS was used to measure the R_h of BSA protein, covalently labeled with the fluorophore Alexa 488, in its native and unfolded states with gradual addition of GO.

2. EXPERIMENTAL SECTION

2.1. Materials and Sample Preparation. Alexa Fluor 488 carboxylic acid, purchased from Invitrogen, was used as received. Bovin serum albumin (BSA) was supplied by Sigma-Aldrich and used without further purification. We used Rhodamine 6G (R6G) as a probe for FLIM, which was bought from Exciton. We synthesized graphene oxide (GO) from graphite powder using the modified Hummer's method.[41,42] Solid GO was dispersed completely in phosphate buffer (pH 7.4, 10 mM) to prepare 1 mg/mL GO solution. We prepared all the required solutions using phosphate buffer of 10 mM (pH 7.4). The structures of all the chemicals used are shown in Scheme 1.

2.2. Adsorption Experiments. We obtained all the adsorption isotherms employing a batch equilibration technique at 25 °C.[39,43] In our present study we performed the adsorption experiments with ten concentration points including a blank sample. To study the effects of different initial protein concentrations on adsorption capacity of a fixed mass of GO, 0.5 mg/mL of GO was incubated with varying concentrations of protein (0−600 mg/L). After that, we centrifuged all the solutions at a speed of 3000 rpm for 15 min. We utilized a UV spectrometer to determine the concentration of the protein employing the Bradford method[44] at 595 nm. The adsorption capacity of adsorbent (mg g^{-1}) at equilibrium q_e was calculated by eq 1.[39,43]

Scheme 1. Structures of (a) BSA (RCSB Protein Data Bank ID: 3V03), (b) Alexa Fluor 488 Carboxylic Acid, TFP Ester, and (c) Rhodamine 6G

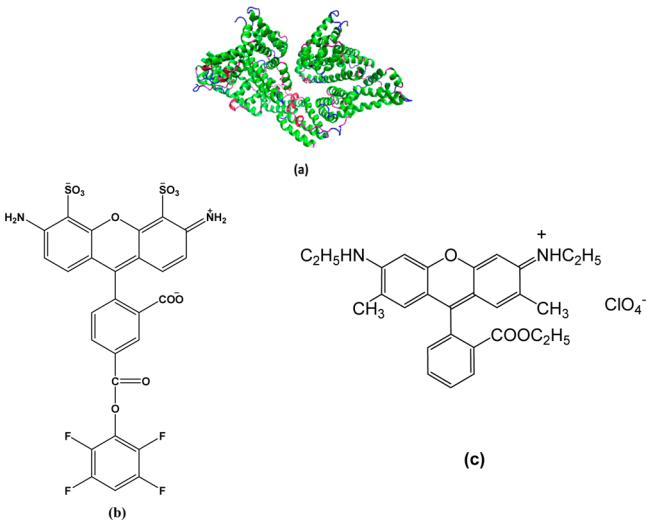

$$q_e = \frac{V(C_0 - C_e)}{m} \quad (1)$$

Here V represents the volume of the solution (in L), c_0 is the initial concentration and c_e is the equilibrium concentration (in mg/L) of BSA in the mixture solution, and m is the mass of the adsorbent (in g).

2.3. Labeling of BSA. In our present study we used Alexa Fluor 488 carboxylic acid TFP ester to label BSA, and we followed the protocol described by the manufacturer (Molecular Probes, Invitrogen). Briefly, the protein solution (2 mg/mL) in 0.1 M sodium bicarbonate was added to the vial of reactive dye, and the reaction mixture was stirred for 1 h at room temperature. We utilized column chromatography using PBS elution buffer (0.1 M potassium phosphate and 1.5 M NaCl) with 2 mM sodium azide (pH 7.2) to separate the labeled protein from free dye. We collected the first colored band, and this contains the labeled protein. Alexa Fluor 488 is covalently attached to the cysteine amino acid part of BSA. There is no unfolding and change in size of the protein after covalent attachment to Alexa Fluor 488.[33,34] We prepared a diluted solution (1 nM) of probe labeled protein by dilution with phosphate buffer (pH 7.4) for our particular FCS study.

2.4. Instrumentation and Methods. The steady-state absorption and fluorescence spectra were recorded with a Shimadzu (model no. UV-2450) UV−vis spectrophotometer and Jobin Yvon-fluorolog spectrofluorometer, respectively. In the fluorescence emission spectroscopy study BSA was excited at 295 nm. We performed atomic force microscopy (AFM) on an Agilent 5500 in the tapping mode. A drop of freshly prepared GO solution was placed on a newly cleaved mica surface, and the sample was spin-coated and air-dried overnight before imaging. A Jasco J-815 CD spectrometer was used to record the near-UV CD spectra at 298 K. For these measurements, a quartz cuvette (path length 10 mm) was used. Each spectrum was obtained by taking the average of three scans and was corrected for the respective blank spectrum. Fourier Transform infrared spectroscopy (FTIR) of the solid GO was recorded using a PerkinElmer instrument (Spectrum RX, serial no 7313) by the KBr pellet method.

Fluorescence Lifetime Imaging Microscopy (FLIM) and Fluorescence Correlation Spectroscopy (FCS). Both the experiments (FLIM and FCS) were carried out using a DCS-120 (complete laser scanning confocal FLIM microscope by Becker & Hickl GmbH) system. The FCS traces were measured using picosecond diode lasers with excitation source connected to inverted microscopes of Zeiss, equipped with a 40× water-immersion objective (NA 1.2). However, for FLIM measurements, 20× objectives had been used. A diode laser of 488 nm, working at continuous-wave (CW) mode (10 mW), was

DOI: 10.1021/acs.langmuir.5b03648
Langmuir 2015, 31, 13793−13801

used for sample excitations, and long pass filters (498 nm) were used to separate the fluorescence signal from the excitation source. The fluorescence signal was collected using two HMP-100-40 GaAsP hybrid detectors, after adjusting the pinhole diameter at 1 mm and maintaining the number of molecules between 5 and 10 in the confocal volume, during each measurement. For all FCS experiments, the final concentration of probe molecules (Alexa Fluor 488-tagged BSA) was 1 nM. However, for FLIM measurements R6G dye was used with a concentration of 10 μM. The instrument response function of the system was less than 100 ps fwhm (full width at half-maximum). In each case images were taken at 15 min interval, and they exhibit the same position for the individual solutions and that confirm proper immobilization of GO and GO−BSA assemblies on the glass surface, and they remained stationary during data acquisition.

In FCS, a very small observation volume (in the order of femtoliters (fL)) is produced inside a sample by making use of the laser and confocal microscopic techniques. The fluctuations in fluorescence intensity, due to the diffusion of fluorescent molecules in and out of the observation volume, can be time-correlated to get a normalized autocorrelation function $G(\tau)$:[35,36]

$$G(\tau) = \frac{\langle \delta F(t)\delta F(t+\tau)\rangle}{\langle F(t)\rangle^2} \tag{2}$$

Here, $\langle F(t)\rangle$ represents the average fluorescence intensity; $\delta F(t)$ and $\delta F(t+\tau)$ give the amount of fluctuation in intensity around the mean value at time t and $(t+\tau)$, respectively, and are given by

$$\delta F(t) = F(t) - \langle F(t)\rangle \tag{3}$$

$$\delta F(t+\tau) = F(t+\tau) - \langle F(t)\rangle \tag{4}$$

$G(\tau)$, the correlation function, can be fitted for a single-component system, where diffusion occurs in only three dimensions in the solution phase, to give the diffusion time (τ_D) according to the equation[35]

$$G(\tau) = \frac{1}{N}\left(1+\frac{\tau}{\tau_D}\right)^{-1}\left(1+\frac{\tau}{\omega^2\tau_D}\right)^{-1/2} \tag{5}$$

where the depth-to-diameter ratio of 3D Gaussian volume is denoted by $\omega = \omega_z/\omega_{xy}$, and N is the number of particles in the observation volume. In case of any fluorescence intensity modulation due to association chemical reaction or conformational change with a relaxation time (τ_R), the correlation function can be written as[36]

$$G(\tau) = \frac{1}{N}\left(1+\frac{\tau}{\tau_D}\right)^{-1}\left(1+\frac{\tau}{\omega^2\tau_D}\right)^{-1/2}(1 + A_1 e^{-\tau/\tau_{R1}} + 1 + A_2 e^{-\tau/\tau_{R2}} + 1 + A_3 e^{-\tau/\tau_{R3}}) \tag{6}$$

where τ_R represents the time of relaxation for an exponential component associated with an amplitude, A. It is considered as a three-component 3D diffusion model.

The diffusion coefficient of the molecule can be calculated from the diffusion time (τ_D) and radius of the observation volume (ω_{xy}) using the equation

$$D_t = \frac{\omega_{xy}^2}{4\tau_D} \tag{7}$$

The calibration of the structural parameter (ω) of the excitation volume was done using a sample having known diffusion coefficient [Rhodamine 6G (R6G) in water, $D_t = 4.14 \times 10^{-6}$ cm^2 s^{-1}] by the given equation.[45,46] The fitted plot is shown in the Supporting Information (Figure S1).

$$G(\tau) = 1 + \frac{1}{N}\left(1+\frac{4D_t\tau}{\omega_{xy}^2}\right)^{-1}\left(1+\frac{4D_t\tau}{\omega^2\omega_{xy}^2}\right)^{-1/2} \tag{8}$$

In the fitting analysis ω_{xy} and ω were kept as free global parameters. From the obtained ω value, V_{eff} is calculated from eq 9.

$$V_{eff} = \pi^{3/2}\omega_{xy}^3\omega \tag{9}$$

From the global analysis of the fluorescence correlation function of R6G of varying concentration, the estimated observation volume is 1.7 fL, with a transverse radius of 283 nm.

The following Stokes−Einstein equation was employed to determine the R_h of the diffusing molecule:[45]

$$R_h = \frac{k_B T}{6\pi\eta D_t} \tag{10}$$

where k_B is the Boltzmann constant, T is the absolute temperature, D_t is the diffusion coefficient, and η is the viscosity of the medium.

3. RESULTS AND DISCUSSION

3.1. Adsorption Isotherm of BSA on GO Surface. Protein adsorption capacity of GO was evaluated for different BSA concentrations in phosphate buffer solution at pH 7.4. GO exhibited the adsorption capacity ~105 mg/g. We can see from Figure 1 the amount of protein adsorbed as a function of the initial concentration of BSA. With increasing initial concentration of BSA, the amount of the protein adsorbed was increased at all conditions. The maximum protein adsorption was observed in the concentration region 288−320 mg/L (Figure 1). The saturation of the binding sites in GO was observed in protein concentrations above 320 mg/L. Thus, further measurements (AFM and FLIM) were performed at 300 mg/L BSA concentration. The surface was found to reach a plateau at moderate protein concentration, suggesting a good affinity of BSA molecules for GO surface. The adsorption of BSA in functionalized multiwall carbon nanotubes (CNTs) was performed by Xing et al.[39] where hydrophobicity of CNTs contributed to the protein adsorption. Thus, the common forces involved in protein adsorption on surfaces of GO are hydrophobic interaction and hydrogen bonding interaction.[11,17] Generally, the hydrophilic residue of BSA forms strong hydrogen bonding with GO. Moreover, the aromatic fragment of BSA leads to significant $\pi-\pi$ stacking and CH$-\pi$ interactions with GO surface. From the molecular dynamics simulation these aromatic residues and graphene surface distances were measured which are very less.[17] Also, the adsorption of GO could be attributed to the abundance of carboxylic acid groups on its surface.[11]

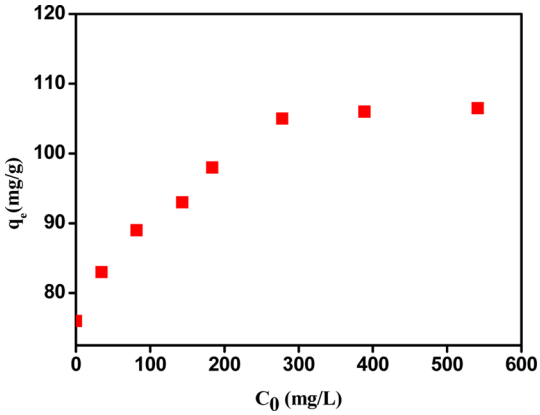

Figure 1. Adsorption isotherms of BSA on graphene oxide (GO) surface.

3.2. Structural Characterization. The synthesized GO was characterized by UV−vis absorption and FTIR presented in Figures S2 and S3 (Supporting Information). The UV−vis

DOI: 10.1021/acs.langmuir.5b03648
Langmuir 2015, 31, 13793−13801

absorption spectrum showed maximum absorption around 229 nm and a shoulder around 300 nm, which is consistent with the previous reports.[47] The shoulder originates due to the $\pi-\pi^*$ transition of C═O groups, and the maxima around 229 nm correspond to the same of aromatic C═C bonds. The FTIR spectrum was utilized to indicate the appearance of different types of oxygen functionalities. The O−H stretching vibration at 3430 cm^{-1}, C═O stretching vibration at 1720 cm^{-1}, skeletal vibrations from unoxidized graphitic domains at 1600 cm^{-1}, C−O (epoxy) stretching vibration at 1220 cm^{-1}, and C−O (alkoxy) stretching vibration at 1050 cm^{-1} confirm the presence of different kinds of oxygen functionalities, and these are almost similar to the previous reports.[48] The AFM images of GO and GO\BSA are displayed in Figure S4 (Supporting Information). The height of the GO sheets obtained from AFM images is 1.2 nm, which confirms that the synthesized GO sheets were single-layered.[18,49] The AFM image in Figure S4a shows the flake nature of GO, which also matches with previous reports.[49] The interaction between GO with biomolecules has been extensively studied earlier by using AFM.[20,13] Adsorption of BSA on GO surface is also shown by AFM in Figure S4b where the average thickness of the BSA grafted onto GO surface is about 4 nm. The AFM results reflect that the BSA molecules are adsorbed on the GO nanosheets. It indicates that the GO nanosheets are suitable supporters for biomacromolecules. The strong hydrophobic interaction between the GO and protein molecules is responsible for this adsorption.

3.3. Fluorescence Lifetime Image. GO has very weak fluorescence, and for real-time observation, it cannot be used directly for fluorescence imaging. The mixture of GO and BSA was coated with R6G dye for the fluorescence lifetime image. Figures 2a and 2b show the intensity and lifetime images of

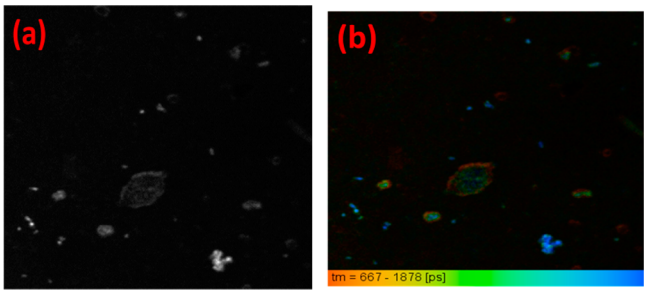

Figure 2. (a) Intensity images and (b) lifetime image of graphene oxide (GO)/BSA.

BSA−GO mixture, respectively. GO sheets are clearly shown in both the images. However, GO sheets are more clearly visible in presence BSA in FLIM mode which is shown in Figure 2b. It is also clearly visible in Figure 2b that BSA molecules are adsorbed on GO surface. Lifetime distribution of R6G in BSA/GO conjugate is demonstrated in this figure. If only GO is coated with R6G, FLIM images are not observed due to GO quenches the R6G fluorescence. Thus, from the FLIM images we can say that there is strong adsorption of BSA on GO sheets. We have discussed earlier that there is hydrophobic interaction between BSA and GO which leads to the adsorption of BSA on GO surface. Through confocal fluorescence lifetime image it can be shown that the herceptin biomolecule adsorbs on the GO surface.[20] Without using any cross-linking reagents, BSA molecules were immobilized onto GO simply by incubating the GO sheets in a phosphate buffer containing BSA.

3.4. Fluorescence Quenching of BSA by GO. In previous reports it was indicated that GO can be used as a widespread fluorescent quencher for peptides and proteins containing tryptophan or tyrosine residues.[19−22] Fluorescence quenching studies of GO on proteins are applicable to BSA, HSA, amyloid beta-40 (Aβ-40), and human islet amyloid polypeptide. A noncovalent interaction is there between the fluorescent amino acids, peptides, proteins, and GO based on their structure and component which affect the fluorescence intensity of the fluorescent assay. We have characterized the fluorescence quenching of BSA by GO with different concentrations, as shown in Figure 3. The fluorescence

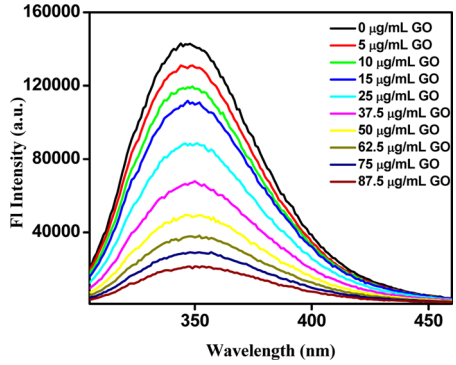

Figure 3. Fluorescence quenching of BSA by mixing with different concentrations of GO.

intensity of BSA assay was significantly reduced after the addition of aqueous solution of GO, but there was hardly any shift of the emission maxima. It is clearly seen that with increment of the GO concentration the emission maxima intensity of BSA dropped significantly. To discuss about the interaction or binding between the fluorescent molecules and GO, it must be considered as an "inner filter effect". As the fluorescence intensity was obtained from the center of a cuvette, we can predict the "inner filter effect" using the equation given as[50,51]

$$F_{obs} = F_{corr} \times 10^{-(A_{ex}d_{ex}/2)-(A_{em}d_{em}/2)} \quad (11)$$

where F_{obs} represents the measured fluorescence intensity, F_{corr} gives the correct fluorescence intensity which is recorded in the absence of inner-filter effect, d_{ex} and d_{em} are the cuvette path length in the excitation and emission direction (in cm), respectively, and A_{ex} and A_{em} represent the measured absorbance values at the excitation and emission wavelength in the presence of compound, respectively. The fluorescence quenching has been followed by the Stern−Volmer equation

$$\frac{F_0}{F} = 1 + K_{SV}[Q] \quad (12)$$

where F_0 and F represent the fluorescence intensities of the probe molecules in the absence and presence of the quencher GO, respectively. We have corrected the values of F_0/F as discussed above using the inner-filter effect. In the above equation, K_{SV} represents the Stern−Volmer constant and [Q] is the concentration of the GO. The probable reason for the observed decrease of fluorescence intensity may be because of the collisional quenching which is proved by many groups. The decrease in the fluorescence intensity after considering the

DOI: 10.1021/acs.langmuir.5b03648
Langmuir 2015, 31, 13793−13801

inner-filter effect indicates that there is a significant fluorescence quenching effect between GO and tryptophan (Trp). The corrected F_0/F vs [Q] plot is shown in Figure 4. It

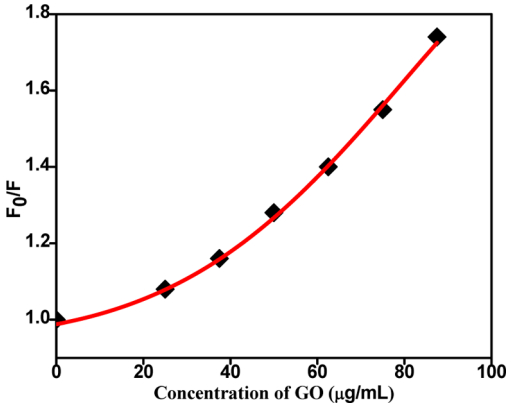

Figure 4. Stern–Volmer plot (F_0/F after inner-filter effect correction vs concentration of quencher) of BSA against the concentration of GO as the quencher.

has been theoretically justified that Trp has a strong adsorption on the graphene surface through $\pi-\pi$ interactions in preferred orientation with respect to the plane of graphene.[52] The concave surface of the GO which is larger surface of GO generally interacts with BSA. However, GO is the oxidized form of graphene in which the edge is occupied by carboxylic acid groups and the basal plane contains hydroxyl and epoxy groups; it also consists of many small aromatic areas with sp^2-hybridized carbons. Therefore, the prominent $\pi-\pi$ interaction or hydrophobic interaction involving GO and Trp or tyrosine (Tyr) plays a vital role for strong fluorescence quenching of BSA.[53,54] The $\pi-\pi$ interactions can exist between the aromatic rings of GO and the indole structure of Trp residues. Conformational changes of proteins because of the GO–protein interactions are other possibilities for the decrease in the fluorescence intensity of BSA.[55,56]

3.5. FCS Studies of Alexa-Labeled BSA. The adsorption behavior of BSA molecules on GO surface is revealed using the steady-state and time-resolved fluorescence measurement. FCS can also be used for the direct measurement of the diffusion of the BSA molecules adsorbed on the GO surfaces. FCS is developed on the time-dependent intensity fluctuations analysis which arises because of some dynamic processes, mainly translational diffusion into and out of observed volume. After gradual addition of GO, BSA molecules are adsorbed on the GO surfaces and that slow down the diffusion of the BSA. The adsorption of the BSA can be confirmed from the diffusion of Alexa Fluor 488-labeled BSA obtained from FCS. FCS autocorrelation of Alexa Fluor 488-labeled BSA with different concentrations of GO in phosphate buffer are provided in Figure 5. The diffusion time (τ_D) was determined from the autocorrelation traces after fitting them to a three-component 3D diffusion model (eq 6). From the value of τ_D, the diffusion coefficient (D_t) was calculated using eq 7, followed by the determination of R_h using the value of τ_D according to eq 10. The diffusion coefficient (D_t) indicates that the mass of the substance diffuses through a unit surface in a unit time. The higher the diffusion coefficient value, the lower the diffusion of the substrate. Free Alexa Fluor 488-labeled BSA has a high D_t value, but after adsorption on GO surface its D_t value decreases

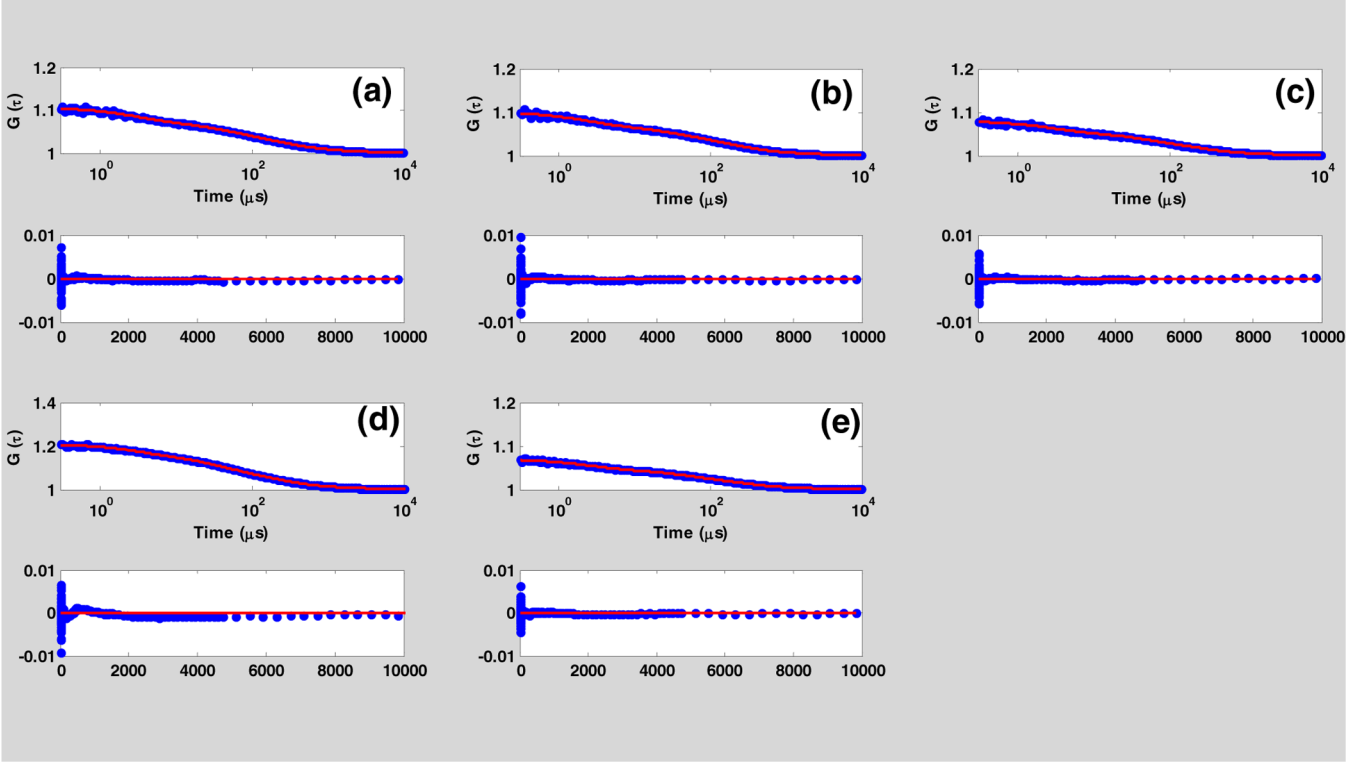

Figure 5. Fluorescence correlation curves of BSA–Alexa 488 with different concentrations of GO: 0.0 (a), 10 (b), 30 (c), 50 (d), and 70 μg/mL (e). The points are the experimental data, and the lines represent best fits. The residuals depicting the quality of the fits are shown at the bottom of each curve.

DOI: 10.1021/acs.langmuir.5b03648
Langmuir 2015, 31, 13793–13801

Table 1. Fitted FCS Data of Alexa 488-Labeled BSA with Different Concentration of Graphene Oxide

systems	τ_D (μs)	τ_{R1} (μs) (A_1)	τ_{R2} (μs) (A_2)	τ_{R3} (μs) (A_3)	D_t[a] (μm^2/s)	R_h[a] (Å)
BSA native	320	3.00 (0.39)	25.04 (0.26)	151.70 (0.35)	83.8	28.7
native BSA + 10 μg/mL GO	335	2.25 (0.40)	22.42 (0.23)	196.30 (0.37)	80.3	30.0
native BSA + 30 μg/mL GO	354	2.70 (0.55)	31.16 (0.20)	233.10 (0.25)	75.9	31.7
native BSA + 50 μg/mL GO	550	3.68 (0.28)	40.44 (0.37)	265.00 (0.35)	48.9	49.3
native BSA + 70 μg/mL GO	650	2.10 (0.36)	3.27 (0.28)	650.00 (0.36)	41.4	58.2

[a]Experimental error ±5%

drastically. D_t, τ_D, and R_h values of Alexa Fluor 488-labeled BSA with different concentrations of GO in phosphate buffer of pH 7.4 have been tabulated in Table 1. From these values, it is clearly observed that the τ_D of the protein is increased after the addition of GO. Fitting of the FCS traces to a three-component 3D diffusion model led to the determination of the three relaxation time components (τ_R) arising from the conformational dynamics of the protein, along with the τ_D. Bhattacharyya et al.[34] also obtained three conformational relaxation time constants for the HSA, and these showed that they are increased upon addition of the RTILs. In the native state of the protein (BSA), the three relaxation time components were ~3.00, 25.04, and 151.70 μs. We summarized the values for all the time components and their corresponding amplitude in Table 1. The two faster components are attributed to the chain dynamics, while the slowest component (151.70 μs) is due to the concerted chain motion or interchain interaction.[24,33,34] With gradual addition of GO, the time components gradually increase. At 50 μg/mL GO, the relaxation time components become ~3.68, 40.44, and 265.00 μs. The result indicates there is significant changes of conformational dynamics of BSA with the addition of GO. The slow relaxation of BSA in the presence of GO indicates the adsorption of BSA on GO surface. In 10 mM phosphate buffer of pH 7.4 native BSA shows a diffusion time of 320 μs, and with addition of GO the value of diffusion time increases. It is shown that at 70 μg/mL GO in phosphate buffer diffusion time of BSA is very high (650 μs). Recently we have investigated the conformational dynamics of BSA in different vesicular system where it is shown that the diffusion time of Alexa-labeled BSA is much greater in the vesicular system than in the buffer.[57] The increase of diffusion times of BSA after addition of GO clearly indicates the adsorption of BSA on GO surface. Again the D_t values slow down compared to free BSA after staking of BSA on GO sheets. It is widely accepted that the protein changes its conformation upon adsorption, and as a result, there occurs contact between some hydrophobic regions and the hydrophobic interface.[19−21]

FCS serves as an effective tool to measure hydrodynamics of biomolecules. The increase in the diffusion time after interacting with GO surface results in an increased R_h of the BSA. The variation of R_h values with the concentration of GO is depicted in Figure 6, and the numerical values are entered in Table 1. The R_h value was obtained as 28.7 Å in buffer solution, after fitting the FCS traces with eq 10. This value is in good agreement with that calculated from the empirical formula for the determination of the R_h value of a native protein as proposed by Wilkins et al.[58] as $R_h = 4.75N^{0.29}$ Å, where N denotes the number of amino acid fragments in the protein. The R_h value of native BSA calculated from this formula is 30.11 Å, which is reasonably comparable to the value determined using our FCS experiment. The interaction with GO surface causes R_h of BSA to increase in all the cases, and an approximately 2-fold increase is observed after addition of 70 μg/mL GO. After interaction with GO surface, the protein undergoes expansion which is implied by the increase in the R_h of BSA. The water structures of BSA are destroyed after interaction (H-bonding) with GO. Chattapadhyay et al.[40] explored the conformational dynamics of BSA labeled with Alexa 488 after addition of urea and arginine. In the case of a completely denatured protein, R_h can be calculated utilizing the relation proposed by Wilkins et al., which is given by $R_h = 2.21N^{0.57}$. For fully denatured BSA ($N \sim 583$) R_h is calculated to be 83.33 Å from this formula. This value is even much greater than the maximum value of R_h obtained when interacting with 70 μg/mL GO (58.2 Å). Thus, it is appeared that GO causes partial unfolding of BSA. The driving force is mainly the H-bonding interaction, a hydrophobic interaction between single BSA molecule and the hydrophobic interface of GO. Through FCS several groups showed the increment of R_h of different proteins such as HSA, cytochrome c, and lysozyme after addition of various types of RTILs.[33,34,36]

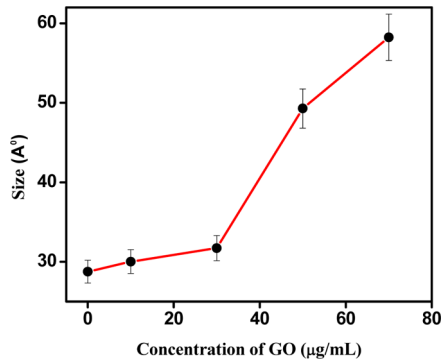

Figure 6. Hydrodynamic radius (R_h) plotted against the different concentrations of GO.

3.6. Circular Dichroism Spectroscopy. The circular dichroism (CD) spectrum in the far-UV region (180−250 nm) is used to probe the secondary structure, conformation, and stability of proteins in solution.[59,60] Thus, it is an important spectroscopic tool for the quantification of the conformational changes of BSA after absorbed onto GO. Two negative bands characteristic of the typical α-helix structure of protein were observed in the CD spectra of BSA at 208 and 222 nm in the ultraviolet region. The negative peaks at 208 and 222 nm correspond to the n → π^* transition due to the peptide bond of an α-helix.[61] The CD spectrum of native BSA and the effect of GO on BSA are exhibited in Figure 7. The CD spectra of BSA with different concentrations of GO were collected after baseline by CD spectra of only the corresponding GO concentration. Using the following equation, the observed CD results were first converted into mean residue ellipticity (MRE).[22]

DOI: 10.1021/acs.langmuir.5b03648
Langmuir 2015, 31, 13793−13801

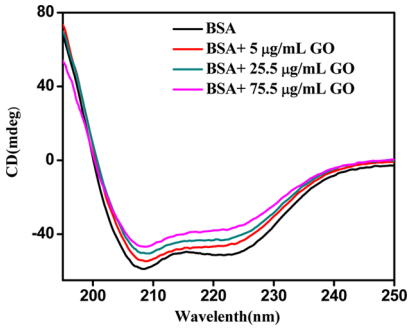

Figure 7. Circular dichroism (far-UV CD) spectra of 5 μM BSA with different concentrations of GO.

$$\text{MRE (deg cm}^2\text{ dmol}^{-1}) = \frac{\theta_{obs}}{C_p n l \times 10} \quad (13)$$

where obs denotes the observed ellipticity in mdeg, C_p denotes the molar concentration of the protein, n represents the number of amino acid residues (583 for BSA), and l is the cell path length (here 0.1 cm). The helicity content of the protein was, then, determined from the calculated MRE values at 208 nm using the equation[22]

$$\%\ \alpha\text{-helix} = \frac{-\text{MRE}_{208} - 4000}{33000 - 4000} \times 100 \quad (14)$$

The estimated α-helicity content of native BSA in phosphate buffer (pH 7.40 and at T = 298 K) comes out to be 55.6%, which agrees reasonably with literature reports.[57] The intensity of α-helix peaks show a gradual declination with increase of GO concentration. The % of the helical content changes from 55.6 to 50.2 at 5 μg/mL GO, to 45.7 at 15 μg/mL GO, and to 41.3 at 75.5 μg/mL GO. The results indicate that conformational changes of BSA were observed after absorbed onto GO surface but not complete unfolding of BSA. The R_h values of BSA calculated from the FCS studies are in well accordance with the CD results. The conformational changes of HSA after addition of GO were shown by Chen and co-workers.[22] Sun et al.[62] showed the conformational transition of Aβ(1−40) peptide after incubation of functionalized GO. The same group also showed that the intensity of the α-helix peak of Aβ(1−40) peptide near 208 nm decreased after addition of functionalized GO. The greatest damage to the structure of BSA is attributed due to GO's influence, and this is mainly resulted from the strong hydrogen bonds and hydrophobic interactions.

4. CONCLUSION

In our particular study, we explored the strong interaction between GO and BSA by adsorption isotherm, fluorescence quenching, CD spectroscopy, AFM, FLIM, and FCS. This particular work reveals that FCS may be employed to explore the influence of GO on diffusion and conformational dynamics of a protein BSA. It is shown that size increases upon addition of GO and slows down the protein dynamics in the native state. Thus, FCS and CD spectroscopic studies give information on conformational changes of BSA after addition of GO. In-depth understanding of the GO−BSA interaction at the single molecular level has been investigated by FLIM and FCS techniques to design more reliable and practical biosensors. FLIM and AFM images clearly reflect adsorption of BSA on the GO surface. Thus, hydrophobic and $\pi-\pi$ stacking interactions between GO and aromatic residues of BSA are found to play a critical role for the adsorption behavior. The fluorescence quenching study indicates that there is strong interaction involving BSA and GO in 10 mM phosphate buffer solution at pH 7.4.

■ ASSOCIATED CONTENT

Supporting Information

The Supporting Information is available free of charge on the ACS Publications website at DOI: 10.1021/acs.langmuir.5b03648.

Measurement of lifetime of FLIM, fitted correlation curve of R6G in water, UV−vis spectra, FTIR spectra, and AFM images of GO and GO−BSA conjugate (PDF)

■ AUTHOR INFORMATION

Corresponding Author

*E-mail nilmoni@chem.iitkgp.ernet.in; Fax 91-3222-255303 (N.S.).

Notes

The authors declare no competing financial interest.

■ ACKNOWLEDGMENTS

N.S. is thankful to SERB, Department of Science and Technology (DST) and Council of Scientific and Industrial Research (CSIR), Government of India, for generous research grants. J.K. is thankful to UGC for a research fellowship. D.B. and N.K. are thankful to IIT Kharagpur and A.R. is thankful to CSIR for research fellowship.

■ REFERENCES

(1) Kam, N. W. S.; Dai, H. Carbon Nanotubes as Intracellular Protein Transporters: Generality and Biological Functionality. *J. Am. Chem. Soc.* **2005**, *127*, 6021−6026.

(2) Cedervall, T.; Lynch, I.; Lindman, S.; Berggård, T.; Thulin, E.; Nilsson, H.; Dawson, K. A.; Linse, S. Understanding the Nanoparticle-Protein Corona Using Methods to Quantify Exchange Rates and Affinities of Proteins for Nanoparticles. *Proc. Natl. Acad. Sci. U. S. A.* **2007**, *104*, 2050−2055.

(3) Yin, Y.; Hu, K.; Grant, A. M.; Zhang, Y.; Tsukruk, V. V. Biopolymeric Nanocomposites with Enhanced Interphases. *Langmuir* **2015**, *31*, 10859−10870.

(4) Hu, K.; Kulkarni, D. D.; Choi, I.; Tsukruk, V. V. Graphene-polymer Nanocomposites for Structural and Functional Applications. *Prog. Polym. Sci.* **2014**, *39*, 1934−1972.

(5) Thompson, A. B.; Calhoun, A. K.; Smagghe, B. J.; Stevens, M. D.; Wotkowicz, M. T.; Hatziioannou, V. M.; Bamdad, C. A Gold Nanoparticle Platform for Protein−Protein Interactions and Drug Discovery. *ACS Appl. Mater. Interfaces* **2011**, *3*, 2979−2987.

(6) Hu, K.; Gupta, M. K.; Kulkarni, D. D.; Tsukruk, V. V. Ultra-robust Graphene Oxide-silk Fibroin Nanocomposite Membranes. *Adv. Mater.* **2013**, *25*, 2301−2307.

(7) Yang, W.; Sun, L.; Weng, J.; Chen, L.; Zhang, Q. Probing the Interaction of Bovine Haemoglobin with Gold Nanoparticles. *IET Nanobiotechnol.* **2012**, *6*, 26−32.

(8) Vangala, K.; Ameer, F.; Salomon, G.; Le, V.; Lewis, E.; Yu, L.; Liu, D.; Zhang, D. Studying Protein and Gold Nanoparticle Interaction Using Organothiols as Molecular Probes. *J. Phys. Chem. C* **2012**, *116*, 3645−3652.

(9) Lu, C. H.; Yang, H. H.; Zhu, C. L.; Chen, X.; Chen, G. N. A graphene Platform for Sensing Biomolecules. *Angew. Chem., Int. Ed.* **2009**, *48*, 4785−4787.

(10) He, S.; Song, B.; Li, D.; Zhu, C.; Qi, W.; Wen, Y.; Wang, L.; Song, S.; Fang, H.; Fan, C. A Graphene Nanoprobe for Rapid, Sensitive, and Multicolor Fluorescent DNA Analysis. *Adv. Funct. Mater.* **2010**, *20*, 453−459.

DOI: 10.1021/acs.langmuir.5b03648
Langmuir 2015, 31, 13793−13801

(11) Park, J. S.; Na, H. K.; Min, D. H.; Kim, D. E. Desorption of single-stranded nucleic acids from graphene oxide by disruption of hydrogen bonding. *Analyst* **2013**, *138*, 1745−1749.
(12) Jang, H.; Kim, Y.-K.; Kwon, H.-M.; Yeo, W.-S.; Kim, D.-E.; Min, D.-H. A Graphene- Based Platform for the Assay of Duplex-DNA Unwinding by Helicase. *Angew. Chem., Int. Ed.* **2010**, *49*, 5703−5707.
(13) Park, J. S.; Goo, N.-I.; Kim, D.-E. Mechanism of DNA Adsorption and Desorption on Graphene Oxide. *Langmuir* **2014**, *30*, 12587−12595.
(14) Pattammattel, A.; Puglia, M.; Chakraborty, S.; Deshapriya, I. K.; Dutta, P. K.; Kumar, C. V. Tuning the Activities and Structures of Enzymes Bound to Graphene Oxide with a Protein Glue. *Langmuir* **2013**, *29*, 15643−15654.
(15) Lu, N.; Yin, D.; Li, Z.; Yang, J. Structure of Graphene Oxide: Thermodynamics versus Kinetics. *J. Phys. Chem. C* **2011**, *115*, 11991−11995.
(16) De, M.; Chou, S. S.; Dravid, V. P. Graphene Oxide as an Enzyme Inhibitor: Modulation of Activity of α-Chymotrypsin. *J. Am. Chem. Soc.* **2011**, *133*, 17524−17527.
(17) Sun, X.; Feng, Z.; Hou, T.; Li, Y. Mechanism of Graphene Oxide as an Enzyme Inhibitor from Molecular Dynamics Simulations. *ACS Appl. Mater. Interfaces* **2014**, *6*, 7153−7163.
(18) Zhang, J.; Zhang, J.; Zhang, F.; Yang, H.; Huang, X.; Liu, H.; Guo, S. Graphene Oxide as a Matrix for Enzyme Immobilization. *Langmuir* **2010**, *26*, 6083−6085.
(19) Li, S.; Aphale, A. N.; Macwan, I. G.; Patra, P. K.; Gonzalez, W. G.; Miksovska, J.; Leblanc, R. M. Graphene Oxide as a Quencher for Fluorescent Assay of Amino Acids, Peptides, and Proteins. *ACS Appl. Mater. Interfaces* **2012**, *4*, 7069−7075.
(20) Zhang, Y.; Wu, C.; Guo, S.; Zhang, J. Interactions of Graphene and Graphene Oxide with Proteins and Peptides. *Nanotechnol. Rev.* **2013**, *2*, 27−45.
(21) Li, S.; Mulloor, J. J.; Wang, L.; Ji, Y.; Mulloor, C. J.; Micic, M.; Orbulescu, J.; Leblanc, R. M. Strong and Selective Adsorption of Lysozyme on Graphene Oxide. *ACS Appl. Mater. Interfaces* **2014**, *6*, 5704−5712.
(22) Ding, Z.; Ma, H.; Chen, Y. Interaction of Graphene Oxide with Human Serum Albumin and Its Mechanism. *RSC Adv.* **2014**, *4*, 55290−55295.
(23) Elson, E. L.; Magde, D. Fluorescence correlation spectroscopy. I. Conceptual basis and theory. *Biopolymers* **1974**, *13*, 1−27.
(24) Webb, W. W. *Single Molecule Spectroscopy in Chemistry, Physics and Biology*; Springer Series in Chemical Physics; Springer GmbH: Berlin, 2010; pp 107−117.
(25) Liu, R.; Hu, D.; Tan, X.; Lu, H. P. Revealing Two-State Protein−Protein Interactions of Calmodulin by Single-Molecule Spectroscopy. *J. Am. Chem. Soc.* **2006**, *128*, 10034−10042.
(26) Tan, X.; Nalbant, P.; Toutchkine, A.; Hu, D.; Vorpagel, E. R.; Hahn, K. M.; Lu, H. P. Single-Molecule Study of Protein−Protein Interaction Dynamics in a Cell Signaling System. *J. Phys. Chem. B* **2004**, *108*, 737−744.
(27) Kim, H. D.; Nienhaus, G. U.; Ha, T.; Orr, J. W.; Williamson, J. R.; Chu, S. Mg^{2+}-dependent conformational change of RNA studied by fluorescence correlation and FRET on immobilized single molecules. *Proc. Natl. Acad. Sci. U. S. A.* **2002**, *99*, 4284−4289.
(28) Kim, J.; Doose, S.; Neuweiler, H.; Sauer, M. The Initial Step of DNA Hairpin Folding: A Kinetic Analysis Using Fluorescence Correlation Spectroscopy. *Nucleic Acids Res.* **2006**, *34*, 2516−2527.
(29) Haldar, S.; Chattopadhyay, K. Interconnection of Salt Induced Hydrophobic Compaction and Secondary Structure Formation Depends on Solution Conditions: Revisiting Early Events of Protein Folding at Single Molecule Resolution. *J. Biol. Chem.* **2012**, *287*, 11546−11555.
(30) Ziv, G.; Thirumalai, D.; Haran, G. Collapse Transition in Proteins. *Phys. Chem. Chem. Phys.* **2009**, *11*, 83−93.
(31) Chattopadhyay, K.; Saffarian, S.; Elson, E. L.; Frieden, C. Measuring Unfolding of Proteins in the Presence of Denaturant Using Fluorescence Correlation Spectroscopy. *Biophys. J.* **2005**, *88*, 1413−1422.
(32) Sherman, E.; Itkin, A.; Kuttner, Y. Y.; Rhoades, E.; Amir, D.; Haas, E.; Haran, G. Using Fluorescence Correlation Spectroscopy to Study Conformational Changes in Denatured Proteins. *Biophys. J.* **2008**, *94*, 4819−4827.
(33) Mojumdar, S. S.; Chowdhury, R.; Chattoraj, S.; Bhattacharyya, K. Role of Ionic Liquid on the Conformational Dynamics in the Native, Molten Globule, and Unfolded States of Cytochrome C: A Fluorescence Correlation Spectroscopy Study. *J. Phys. Chem. B* **2012**, *116*, 12189−12198.
(34) Sasmal, D. K.; Mondal, T.; Mojumdar, S. S.; Choudhury, A.; Banerjee, R.; Bhattacharyya, K. An FCS Study of Unfolding and Refolding of CPM-Labeled Human Serum Albumin: Role of Ionic Liquid. *J. Phys. Chem. B* **2011**, *115*, 13075−13083.
(35) Yadav, R.; Sengupta, B.; Sen, P. Conformational Fluctuation Dynamics of Domain I of Human Serum Albumin in the Course of Chemically and Thermally Induced Unfolding Using Fluorescence Correlation Spectroscopy. *J. Phys. Chem. B* **2014**, *118*, 5428−5438.
(36) Pabbathi, A.; Ghosh, S.; Samanta, A. FCS Study of the Structural Stability of Lysozyme in the Presence of Morpholinium Salts. *J. Phys. Chem. B* **2013**, *117*, 16587−16593.
(37) Sarkar, S.; Chattopadhyay, K. Studies of Early Events of Folding of a Predominately β-Sheet Protein Using Fluorescence Correlation Spectroscopy and Other Biophysical Methods. *Biochemistry* **2014**, *53*, 1393−1402.
(38) Chattopadhyay, K.; Elson, E. L.; Frieden, C. The kinetics of conformational fluctuations in an unfolded protein measured by fluorescence methods. *Proc. Natl. Acad. Sci. U. S. A.* **2005**, *102*, 2385−2389.
(39) Du, P.; Zhao, J.; Mashayekhi, H.; Xing, B. Adsorption of Bovine Serum Albumin and Lysozyme on Functionalized Carbon Nanotubes. *J. Phys. Chem. C* **2014**, *118*, 22249−22257.
(40) Ghosh, R.; Sharma, S.; Chattopadhyay, K. Effect of Arginine on Protein Aggregation Studied by Fluorescence Correlation Spectroscopy and Other Biophysical Methods. *Biochemistry* **2009**, *48*, 1135−1143.
(41) Hummers, W. S., Jr.; Offeman, R. E. Preparation of graphitic oxide. *J. Am. Chem. Soc.* **1958**, *80*, 1339.
(42) Kulkarni, D. D.; Choi, I.; Singamaneni, S. S.; Tsukruk, V. V. Graphene Oxide Polyelectrolyte Nanomembranes. *ACS Nano* **2010**, *4*, 4667−4676.
(43) Smith, S. C.; Ahmed, F.; Gutierrez, K. M.; Rodrigues, D. F. A comparative Study of Lysozyme Adsorption with Graphene, Grapheme Oxide, and Single-Walled Carbon Nanotubes: Potential Environmental Applications. *Chem. Eng. J.* **2014**, *240*, 147−154.
(44) Bradford, M. M. Rapid and Sensitive Method for Quantitation of Microgram Quantities of Protein Utilizing Principle of Protein-Dye Binding. *Anal. Biochem.* **1976**, *72*, 248−254.
(45) Müller, C. B.; Loman, A.; Pacheco, V.; Koberling, F.; Willbold, D.; Richtering, W.; Enderlein, J. Precise Measurement of Diffusion by Multi-Color Dual-Focus Fluorescence Correlation Spectroscopy. *Europhys. Lett.* **2008**, *83*, 46001−46005.
(46) Pal, N.; Verma, S. D.; Singh, M. K.; Sen, S. Fluorescence Correlation Spectroscopy: An Efficient Tool for Measuring Size, Size-Distribution and Polydispersity of Microemulsion Droplets in Solution. *Anal. Chem.* **2011**, *83*, 7736−7744.
(47) Li, S.; Aphale, A. N.; Macwan, I. G.; Patra, P. K.; Gonzalez, W. G.; Miksovska, J.; Leblanc, R. M. Graphene Oxide as a Quencher for Fluorescent Assay of Amino Acids, Peptides, and Proteins. *ACS Appl. Mater. Interfaces* **2012**, *4*, 7069−7075.
(48) Choi, E. Y.; Han, T. H.; Hong, J.; Kim, J. E.; Lee, S. H.; Kim, H. W.; Kim, S. O. Noncolvalent Functionalization of Graphene with End-Functional Polymers. *J. Mater. Chem.* **2010**, *20*, 1907−1912.
(49) Yu, L.; Wu, H.; Wu, B.; Wang, Z.; Cao, H.; Fu, C.; Jia, N. Magnetic Fe_3O_4-Reduced Graphene Oxide Nanocomposites-Based Electrochemical Biosensing. *Nano-Micro Lett.* **2014**, *6*, 258−267.
(50) van de Weert, M.; Stella, L. Fluorescence quenching and ligand binding: A critical discussion of a popular methodology. *J. Mol. Struct.* **2011**, *998*, 144−150.

DOI: 10.1021/acs.langmuir.5b03648
Langmuir 2015, 31, 13793−13801

(51) Lakowicz, J. R. *Principles of Fluorescence Spectroscopy*, 3rd ed.; Springer: New York, 2006; pp 56, 278−281.
(52) Rajesh, C.; Majumder, C.; Mizuseki, H.; Kawazoe, Y. A theoretical study on the interaction of aromatic amino acids with graphene and single walled carbon nanotube. *J. Chem. Phys.* **2009**, *130*, 124911−124916.
(53) Lerf, A.; He, H.; Forster, M.; Klinowski, J. Structure of Graphite Oxide Revisited. *J. Phys. Chem. B* **1998**, *102*, 4477−4482.
(54) Zhang, M.; Yin, B.-C.; Wang, X.-F.; Ye, B.-C. Interaction of Peptides with Graphene Oxide and its Application for Real-Time Monitoring of Protease Activity. *Chem. Commun.* **2011**, *47*, 2399−2401.
(55) Cai, W.; Piner, R. D.; Stadermann, F. J.; Park, S.; Shaibat, M. A.; Ishii, Y.; Yang, D.; Velamakanni, A.; An, S. J.; Stoller, M.; An, J.; Chen, D.; Ruoff, R. S. Synthesis and solid-state NMR structural characterization of ^{13}C-labeled graphite oxide. *Science* **2008**, *321*, 1815−1817.
(56) Themistou, E.; Singh, I.; Shang, C.; Balu-Iyer, S. V.; Alexandridis, P.; Neelamegham, S. Application of Fluorescence Spectroscopy to Quantify Shear-Induced Protein Conformation Change. *Biophys. J.* **2009**, *97*, 2567−2576.
(57) Banerjee, C.; Roy, A.; Kundu, N.; Banik, D.; Sarkar, N. New Strategy to Form Giant Vesicles: A Study of Protein Dynamics in Crowded Environment Using Fluorescence Correlation Spectroscopic Technique. *J. Phys. Chem. B* **2015**, submitted for publication.
(58) Wilkins, D. K.; Grimshaw, S. B.; Receveur, V.; Dobson, C. M.; Jones, J. A.; Smith, L. J. Hydrodynamic Radii of Native and Denatured Proteins Measured by Pulse Field Gradient NMR Techniques. *Biochemistry* **1999**, *38*, 16424−16431.
(59) Moriyama, Y.; Takeda, K. Protective Effects of Small Amounts of Bis(2-ethylhexyl)sulfosuccinate on the Helical Structures of Human and Bovine Serum Albumins in Their Thermal Denaturations. *Langmuir* **2005**, *21*, 5524−5528.
(60) Parker, W.; Song, P. S. Protein Structures in SDS Micelle-Protein Complexes. *Biophys. J.* **1992**, *61*, 1435−1439.
(61) Kamat, B. P.; Seetharamappa, J. In vitro Study on the Interaction of Mechanism of Tricyclic Compounds with Bovine Serum Albumin. *J. Pharm. Biomed. Anal.* **2004**, *35*, 655−664.
(62) Qing, G.; Zhao, S.; Xiong, Y.; Lv, Z.; Jiang, F.; Liu, Y.; Chen, H.; Zhang, M.; Sun, T. Chiral Effect at Protein/graphene Interface: A Bioinspired Perspective to Understand Amyloid Formation. *J. Am. Chem. Soc.* **2014**, *136*, 10736−10742.

DOI: 10.1021/acs.langmuir.5b03648
Langmuir 2015, 31, 13793−13801